

Heterozygous Variants in *KDM4B* Lead to Global Developmental Delay and Neuroanatomical Defects

Anna R. Duncan,¹ Antonio Vitobello,^{2,3,4} Stephan C. Collins,³ Valerie E. Vancollie,⁵ Christopher J. Lelliott,⁵ Lance Rodan,^{6,7} Jiahai Shi,⁸ Ann R. Seman,⁶ Emanuele Agolini,⁹ Antonio Novelli,⁹ Paolo Prontera,¹⁰ Maria J. Guillen Sacoto,¹¹ Teresa Santiago-Sim,¹¹ Aurélien Trimouille,¹² Cyril Goizet,¹³ Mathilde Nizon,¹⁴ Ange-Line Bruel,^{2,3} Christophe Philippe,^{2,3} Patricia E. Grant,^{1,15} Monica H. Wojcik,^{1,6} Joan Stoler,⁶ Casie A. Genetti,^{6,16} Marieke F. van Dooren,¹⁷ Saskia M. Maas,¹⁸ Marielle Alders,¹⁸ Laurence Faivre,^{2,3,4} Arthur Sorlin,^{2,3,4,19} Grace Yoon,²⁰ Binnaz Yalcin,^{3,*} and Pankaj B. Agrawal^{1,6,16,*}

Summary

KDM4B is a lysine-specific demethylase with a preferential activity on H3K9 tri/di-methylation (H3K9me_{3/2})-modified histones. H3K9 tri/di-demethylation is an important epigenetic mechanism responsible for silencing of gene expression in animal development and cancer. However, the role of *KDM4B* on human development is still poorly characterized. Through international data sharing, we gathered a cohort of nine individuals with mono-allelic *de novo* or inherited variants in *KDM4B*. All individuals presented with dysmorphic features and global developmental delay (GDD) with language and motor skills most affected. Three individuals had a history of seizures, and four had anomalies on brain imaging ranging from agenesis of the corpus callosum with hydrocephalus to cystic formations, abnormal hippocampi, and polymicrogyria. In mice, lysine demethylase 4B is expressed during brain development with high levels in the hippocampus, a region important for learning and memory. To understand how *KDM4B* variants can lead to GDD in humans, we assessed the effect of *KDM4B* disruption on brain anatomy and behavior through an *in vivo* heterozygous mouse model (*Kdm4b*^{+/-}), focusing on neuroanatomical changes. In mutant mice, the total brain volume was significantly reduced with decreased size of the hippocampal dentate gyrus, partial agenesis of the corpus callosum, and ventriculomegaly. This report demonstrates that variants in *KDM4B* are associated with GDD/ intellectual disability and neuroanatomical defects. Our findings suggest that *KDM4B* variation leads to a chromatinopathy, broadening the spectrum of this group of Mendelian disorders caused by alterations in epigenetic machinery.

Global developmental delay (GDD) affects 1%–3% of children less than 5 years old, and a similar rate of intellectual disability (ID) is present in older children.¹ Taken together, GDD and ID are a worldwide pediatric public health problem with a lifetime care cost of up to \$1,000,000 per child.² GDD and ID are often associated with other developmental disorders of childhood and can lead to increased caregiver stress.^{1,3} The causes of GDD/ID are multifactorial; data suggest that a majority of cases are secondary to a genetic cause.^{1,4} For example, in severe ID, an estimated 62% of cases are secondary to *de novo* variants.^{4,5} A genetic diagnosis can be extraordinarily important for a family to know; it can empower parents to advocate for their child

and provide them with prognosis, validation, social support, educational services, and an understanding of reoccurrence risk.^{1,6} Our understanding of GDD/ID continues to evolve with the advancements in sequencing technologies and functional modeling leading to identification of novel genes and associated pathogenic variants. Using exome sequencing (ES), we have identified a cohort of nine individuals with GDD and heterozygous variants in *KDM4B*.

KDM4B (MIM: 609765, alternative name JMJD2B) is a lysine-specific histone demethylase with a catalytic activity against different histone modifications, including H3K9me₃, H3K9me₂, H3K36me₃, H3K36me₂, H4K20me₂, and H1.4K26me₃. H3K9me_{3/2} is the preferred substrate

¹Division of Newborn Medicine, Department of Pediatrics, Boston Children's Hospital, Boston, MA 02115, USA; ²Unité Fonctionnelle Innovation en Diagnostic Génomique des Maladies Rares, FHU-TRANSLAD, CHU Dijon Bourgogne, 21000 Dijon, France; ³INSERM UMR1231 GAD, Université de Bourgogne Franche-Comté, 21000 Dijon, France; ⁴Centre de Référence Maladies Rares « Anomalies du Développement et Syndromes Malformatifs », Centre de Génétique, FHU-TRANSLAD, CHU Dijon Bourgogne, 21000 Dijon, France; ⁵Wellcome Sanger Institute, Hinxton, Cambridge CB10 1SA, UK; ⁶Division of Genetics and Genomics, Boston Children's Hospital, Boston, MA 02115, USA; ⁷Department of Neurology, Boston Children's Hospital, Boston, MA 02115, USA; ⁸Department of Biomedical Sciences, City University of Hong Kong, Hong Kong, Hong Kong SAR; ⁹Laboratory of Medical Genetics Unit, Bambino Gesù Children's Hospital, 00146 Rome, Italy; ¹⁰Medical Genetics Unit, Maternal-Infantile Department, Hospital and University of Perugia, 06129 Perugia, Italy; ¹¹Clinical Genomics Program, GeneDx, Gaithersburg, MD 20877, USA; ¹²Department of Medical Genetics, University Hospital of Bordeaux, 33076 Bordeaux, France; ¹³Reference Center for Neurogenetics, Department of Medical Genetics, University Hospital of Bordeaux, 33076 Bordeaux, France; ¹⁴CHU Nantes, Genetic Medical Department, 44093 Nantes, France; ¹⁵Department of Radiology, Boston Children's Hospital, Boston, MA 02115, USA; ¹⁶The Manton Center for Orphan Disease Research, Boston Children's Hospital, Boston, MA 02115, USA; ¹⁷Department of Clinical Genetics, Erasmus MC University Medical Center Rotterdam, PO Box 2040, 3000 CA Rotterdam, the Netherlands; ¹⁸Amsterdam UMC, University of Amsterdam, Department of Clinical Genetics, Meibergdreef 9, 1105 AZ Amsterdam, the Netherlands; ¹⁹Centre de Référence Maladies Rares « Déficiences Intellectuelles de Causes Rares », Centre de Génétique, FHU-TRANSLAD, CHU Dijon Bourgogne, 21000 Dijon, France; ²⁰Divisions of Neurology and Clinical and Metabolic Genetics, Department of Paediatrics, The Hospital for Sick Children, University of Toronto, Toronto, ON M5G 1X8, Canada

*Correspondence: binnaz.yalcin@inserm.fr (B.Y.), pagrawal@enders.tch.harvard.edu (P.B.A.)

<https://doi.org/10.1016/j.ajhg.2020.11.001>

© 2020 American Society of Human Genetics.

that is enriched at constitutive and facultative heterochromatin, localized at pericentromeric and telomeric regions as well as at nuclear lamina in mammalian cells.⁷ Accumulation of H3K9 methylation is associated with chromatin compaction and gene repression.⁸ Previous studies of *KDM4B* have primarily been in cancer models and have shown that *KDM4B* is strongly regulated by multiple cellular stimuli, including oxygen concentration and Hif1 alpha, androgens, estrogen, and DNA damage.^{9–14}

Recent data suggest that *KDM4B* is expressed during brain development with high expression in the hippocampus, a region important for learning and memory.¹⁵ In a neuron-specific *KDM4B* (*JMJD2B*)-deficient mouse model, its depletion was associated with an increase in total dendritic spine number within the hippocampus and a notable decrease in maturity of the dendritic spines. These mice also exhibited hyperactive behavior, had deficits in their working memory, and were prone to seizures.¹⁵ This study suggests that *KDM4B* depletion alters connectivity, particularly within the hippocampus. Several other histone lysine demethylases have previously been linked to neurodevelopmental disorders, including *KDM5C*, which causes an X-linked intellectual disability syndrome, and *KDM6A*, which has been implicated in Kabuki syndrome.^{16,17} In the case of *KDM5C*, its depletion is thought to lead to altered dendritic development in the rodent cerebellar cortex, while haploinsufficiency of *KDM6A* in Kabuki syndrome is thought to affect neural differentiation.^{16,18} However, the role of *KDM4B* in human development has not been investigated.

We identified a cohort of nine individuals with extremely rare variants in *KDM4B* and presenting with syndromic GDD/ID and neuroanatomical findings. Using a heterozygous mouse model (*Kdm4b*^{+/-}), we performed a systematic assessment of brain regions to analyze neuroanatomical defects in this model and identified structural anomalies compatible with those identified in our cohort. Overall, this study highlights the importance of *KDM4B* in human brain development and cognitive function.

We performed trio ES on an individual (I:2) who presented with GDD, agenesis of the corpus callosum, intracranial cysts leading to obstructive hydrocephalus, seizures, abnormal hippocampi, and dysmorphic facial features (Tables 1, S1, and S2) and identified a *de novo* missense variant in *KDM4B*. International data sharing through MatchMaker Exchange allowed us to identify eight additional individuals carrying rare missense variants in this gene with an overlapping clinical spectrum (Figure 1A; Table 1). In order to better delineate the symptomatology associated with *KDM4B* variation, we first compared the clinical features and MRIs of each of the individuals identified. All were diagnosed with GDD and/or ID and language and gross motor skills were found to be the most affected; language delay was present in eight out of nine and gross motor delay was present in six out of nine of the individuals. Three of the individuals (I:2, I:4, and I:7) had a history of seizures, and four of them

(I:1, I:2, I:5, and I:7) had structural anomalies appreciated on their brain MRIs ranging from agenesis of the corpus callosum with hydrocephalus to cystic formations, polymicrogyria, and abnormal formation of the hippocampus (Figure 2). Only one of the individuals (I:6) was microcephalic. Dysmorphic features were present in this cohort as well, including abnormal palpebral fissures, short philtrum, sparse hair, and clinodactyly (Table S1).

Seven of the individuals (I:1–I:5, I:7, and I:8) harbored *de novo* variants, while two (I:6 and I:9) inherited them from affected parents. Four of the variants were missense, three were frameshift, one was a single synonymous substitution predicted to lead to a splicing defect, and one was a canonical splicing variant leading to loss of function (Figures 1A and S1). The combined annotation dependent depletion (CADD) scores of the missense variants ranged from 25.4 to 32, and all identified variants were absent from gnomAD, including the inherited variants from I:6 and I:9, which were identified through this study.¹⁹ According to data from gnomAD, *KDM4B* has a significantly reduced number of truncating and missense variants in controls, indicating a constraint on both types of variants in a control population (probability of being loss-of-function intolerant [pLi] = 1, Z score for missense variants = 3.48).

Molecular modeling was computed to assess how variants in *KDM4B* would affect the protein's structure and function. None of the missense variants showed a predicted effect on splicing. *KDM4B* has five domains, which include two jumonji catalytic demethylase domains, one is the N-terminal portion (JmjN) and one is the C-terminal portion (JmjC) domain; a double tudor domain; and two plant homeodomains (PHDs). The JmjC domain is the catalytic domain of the protein, while the JmjN domain helps to provide essential structure. The tudor domain binds the histones, H3K23me2/3, allowing for demethylation.²⁰ The PHDs contain zinc fingers, which are important for *KDM4B*'s ability to interact with the chromatin as well. The variant in I:1, p.Pro1095Leu, is located at the tail of *KDM4B*, which is a flexible region (Figure 1A). This variant may not impair the structure of *KDM4B*, but it may alter *KDM4B*'s interactions with binding partners. The variant in I:2, p.His768Arg, is predicted to destabilize the zinc knuckle that connects the two zinc fingers within the PHD. This prediction is based on the structural similarity between the zinc fingers of *KDM4B* and the BRPF1. His768 has a similar localization in *KDM4B* to His300 in BRPF1. His300 forms a close contact with a zinc molecule and is important for the zinc knuckle structure. Because His768 plays a similar role in *KDM4B*, the introduction of arginine will most likely break the contact formed with zinc, destabilizing the zinc knuckle structure as well (Figure 1B). The variants in I:3 and I:7, p.Leu220Pro and p.Arg222Trp, respectively, are both located within the catalytic, JmjC domain. In I:3, the substitution of leucine for proline will destroy the local helical structure of the catalytic domain, most likely impairing *KDM4B* catalytic function (Figure 1B[1a and 1b]). In I:7, arginine is substituted

Table 1. Clinical and Genetic Findings of Individuals with KDM4B Variants

Affected Individual (I)/ Country	I:1 (Italy)	I:2 (USA)	I:3 (Netherlands)	I:4 (Netherlands)	I:5 (France)	I:6 (France)	I:7 (Canada)	I:8 (France)	I:9 (France)
Variant from reference sequence: NM_015015.2	c.3284C>T (p.Pro1095Leu)	c.2303A>G (p.His768Arg)	c.659T>C (p.Leu220Pro)	c.288C>T (r.287_317del; p.Glu97Thrfs*66); synonymous variant leading to new donor splice site and frameshift	c.2221dup (p.Glu741Glyfs*41)	c.1778_1779delAG (p.Glu593Glyfs*41)	c.664C>T (p.Arg222Trp)	c.371_374del (p.Lys124Thrfs*48)	c.1907–1G>C (p.?)
gnomAD frequency	0	0	0	0	0	0	0	0	0
CADD score	25.4	25.6	32	–	–	–	32	–	–
Inheritance	<i>de novo</i>	<i>de novo</i>	<i>de novo</i>	<i>de novo</i>	<i>de novo</i>	paternally inherited	<i>de novo</i>	<i>de novo</i>	maternally inherited
Sex	male	male	female	male	male	female	female	male	male
Family history	NC	parents from Middle East and consanguineous	NC	NC	NC	father with learning disabilities	NC	mother and father with mild learning disabilities	mother with a similar phenotype
Gross motor delay	+	+	+	+	+	–	+	–	–
Fine motor delay	+	+	–	–	–	–	+	+	–
Language delay	+	+	+	+	+	+	+	+	–
GDD or ID	+, GDD	+, GDD	+, GDD	+, GDD	+, GDD and mild ID	+, GDD and severe ID, IQ = 50	+, GDD	+, GDD and mild ID, IQ 60–72	+, mild ID
Tone	hypotonia	ND	ND	ND	ND	ND	central hypotonia, peripheral hypertonia	facial hypotonia	ND
Seizures	–	+, neonatal seizures, none since then	–	+, seizures starting at 2.5 years	–	–	+, history of infantile spasms starting at 3 weeks	–	–
Behavioral concerns	ND	ADHD	behavior concerns, autistic features	ND	history of intermittent aggression with other children	eating disorder; compulsive behavior	ND	aggression, ADHD	–
Other neurological abnormalities	–	+, obstructive hydrocephalus s/p shunt placement	+, ataxia, autistic features	–	+, general clumsiness	–	–	–	–

Abbreviations: +, features are present; –, features are absent; NC, noncontributory; ND, not documented.

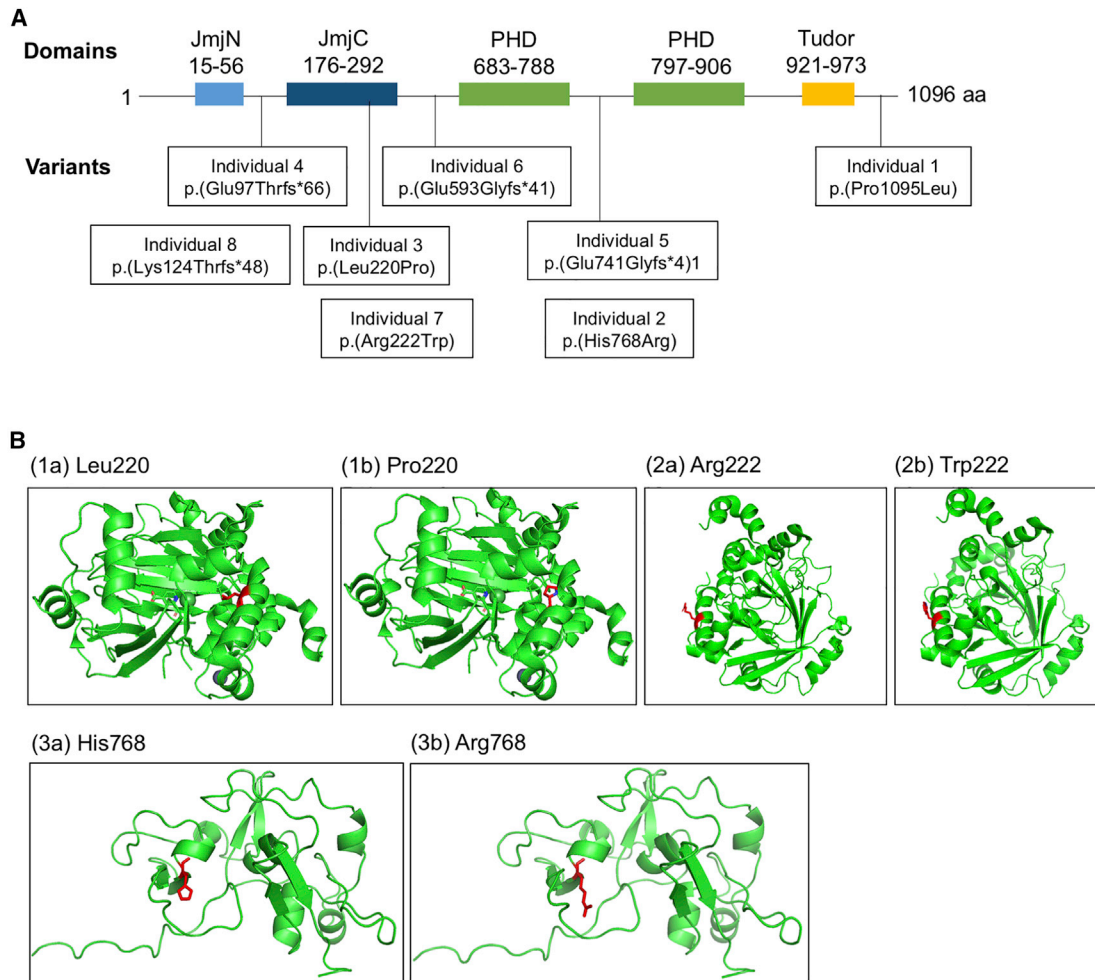


Figure 1. KDM4B Variant Localization and Molecular Modeling

(A) KDM4B with domains and patient individual variants noted.

(B) Molecular modeling of the missense variants in individuals (I) 2, 3, and 7. (1a) shows the helix formed by the catalytic domain of KDM4B. Residue Leu220 is in red. (2b) shows the local destruction of the helical structure when Pro220 is substituted. Pro220 is shown in red. (2a) shows the residue Arg222 within the catalytic domain of KDM4B; Arg222 is highlighted in red. (2b) shows the substitution of Arg222 for Trp222 in I:7, which creates a bulky hydrophobic side chain most likely altering the folding and stability of the helix formation; Trp222 is shown in red. (3a) shows His768 and the zinc knuckle formation; His768 highlighted in red. (3b) shows the unraveling of the zinc knuckle with the substitution of Arg768 in I:2; Arg768 is shown in red.

for tryptophan on the outside of the protein, creating a bulky hydrophobic side chain, which most likely alters the folding and stability of the helix (Figure 1B). The molecular modeling overall suggests that missense variants in *KDM4B* lead to loss or reduction of KDM4B function.

We then assessed how *KDM4B* disruption impacts brain anatomy and behavior through a mouse model, with a focus on the size and shape of the brain structures. Mouse mutants were generated with the knockout-first allele method.²¹ The strategy relies on the identification of an exon common to all transcript variants (exon 5), upstream of which a LacZ cassette was inserted. Exon 5 of the *Kdm4b* allele was flanked by *loxP* sequences bilaterally (Figure 3A). The resulting *Kdm4b^{tm1a(EUCOMM)Wtsi}* mice were then phenotyped.

At weaning age, mouse survival was assessed from 142 successfully genotyped mice originating from several

different litters and derived from a heterozygous-by-heterozygous breeding scheme. We obtained the expected number of wild type (WT) and heterozygous *Kdm4b^{+/-}* mice, but only five (3%) were homozygous and all were female mice, suggesting that the *tm1a* allele of *Kdm4b* is not compatible with life in males. To determine the window of death, we carried out a recessive lethality screen at mouse embryonic day 14.5 (E14.5). The rate of homozygosity was, as expected, 22.2% (eight out of 36 embryos assessed).

The reason underlying embryonic lethality in the homozygous knockout mice is unknown and will require further studies; however, these preliminary data suggest death's occurring late during development between E14.5 and weaning age. Male and female *Kdm4b^{+/-}* mice were then studied independently. The weights of *Kdm4b^{+/-}* mice did not significantly differ from their litter-matched controls (Table S3). In line with this, there were no significant

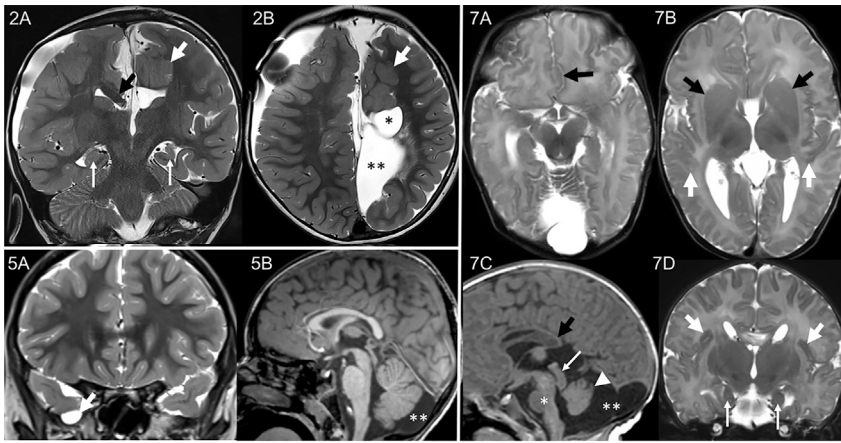


Figure 2. MRI Findings in Individuals 2, 5, and 7

I:2 had many abnormalities, including agenesis of the corpus callosum with a right bundle of Probst (2A, black arrow), white matter cysts (2B, asterisk), interhemispheric cysts (2B, two asterisks), polymicrogyria (2A and 2B, white arrows), and incompletely rotated dysmorphic hippocampi with the left decreased in volume (2A, thin arrows). The following are not shown: absent left fornix with right fornix fused with the bundle of Probst, subcortical gray matter heterotopia, stenogrya of the right hemisphere (probably due to prior hydrocephalus), and decreased white matter volume. I:5 had a small right middle cranial fossa meningocele (5A, arrow) and mega cisterna magna (5B, two asterisks). I:7 also had

many abnormalities, including partial agenesis of the corpus callosum (7C, black arrow), polymicrogyria (7B and 7D, arrows), dysmorphic hippocampi (7D, thin arrows), interdigitation of the frontal lobes (7A, arrow), fused caudate and lentiform nuclei with absent anterior limb internal capsule (7B, arrows), mega cisterna magna (7C, two asterisks), prominent tectum (7C, arrow), incompletely rotated small vermis (7C, arrowhead), and hypoplastic brainstem (7C, asterisk). The following are not shown: dysmorphic partially fused fornices, azygous ACA, small optic nerves, and small cerebellar hemispheres.

differences when comparing to a set of 771 baseline controls accumulated over a 1 year period (Figure 3F; Table S4).

Using a recently developed robust approach for the assessment of 63 brain parameters across 15 distinct brain regions, we analyzed neuroanatomical defects in adult *Kdm4b*^{+/-} mice.²² This consisted of a systematic quantification of the same coronal brain regions at Bregma +0.98 mm and Bregma -1.34 mm, as well as an additional coronal section at Bregma -2.06 mm, to further characterize the hippocampus and the corpus callosum. To minimize variation due to sex and age, we only used male mice aged 16 weeks for analysis. In the het mice, a large number of neuroanatomical parameters were reduced in size when compared to WTs with the exception of the ventricles, which were enlarged in size by 92% ($p = 0.009$) (Figures 3B and 3C). The total brain area parameter was significantly reduced by 13.8% ($p = 0.0005$) concomitantly with smaller size of the dentate gyrus of the hippocampus (-25.3%, $p = 6.9E-5$) and decreased height of the soma of the corpus callosum (-24.7%, $p = 0.01$). At Bregma -2.06 mm, the small size of the dentate gyrus was confirmed and interestingly the corpus callosum was absent (Figures 3D and 3E, Table S5), indicating corpus callosum agenesis. Taken together, these results suggest a contribution of *Kdm4b* in the regulation of the size of the brain, the hippocampus, and the corpus callosum while contributing to ventriculomegaly.

We also assessed whether haploinsufficiency of *Kdm4b* could lead to behavioral abnormalities in a similar way to the neuronal conditional homozygous knockout of *Jmjd2b* (*Kdm4b*).¹⁵ Although open-field findings showed an overall increase of 20% in traveled distance between 2 to 4 min in the het mice, this hyperactive behavior was not statistically significant (Figures 3G-3K).

In this study, we have identified nine individuals with extremely rare variants in *KDM4B* and syndromic GDD.

We have shown an overlap in the neuroanatomical features of the het mice in our murine model with our clinical cohort. In at least two of the three individuals in the study for whom we could obtain MRI images, the MRIs closely mirrored the alterations seen in the het mouse cortex with agenesis of the corpus callosum and dysmorphic hippocampi present. The remaining MRIs were reported as normal, although we were unable to obtain the images for formal review. Molecular modeling of the missense variants suggests that these variants lead to altered *KDM4B* folding, stability, catalytic activity, and ultimately, loss or reduction of function. Because *KDM4B* is a histone modifier that acts through lysine demethylation, we hypothesize that the transcription of target genes regulating brain anatomy, in particular the morphology of the hippocampus and the corpus callosum, are suppressed in a dose-dependent manner. The mouse model therefore consistently shows neuroanatomical difference, whereas the human cohort shows a range of severity most likely secondary to the degree of *KDM4B* haploinsufficiency.

Emerging data suggest that variants in chromatin modifiers are an important cause of neurodevelopmental disability ranging from intellectual disability to autism and schizophrenia.²³⁻²⁶ Variants in lysine demethylases (KDMs) and lysine methyltransferases (KMTs), in particular, are predicted to cause 22 different developmental delay syndromes.²⁷ These epigenetic modifications can affect the future plasticity of neuronal networks, altering a person's ability to learn and remember.²⁸ Further understanding of these mechanisms provides important insights into neurogenesis and the broad field of developmental disorders. A previous report on neuron-specific *Kdm4b* (*Jmjd2b*) knockout mice by Fukiwara et al. shows that *KDM4B* (*JMJD2B*) depletion in mice leads to alteration in dendritic spines within the hippocampi.¹⁵ Dendritic spine

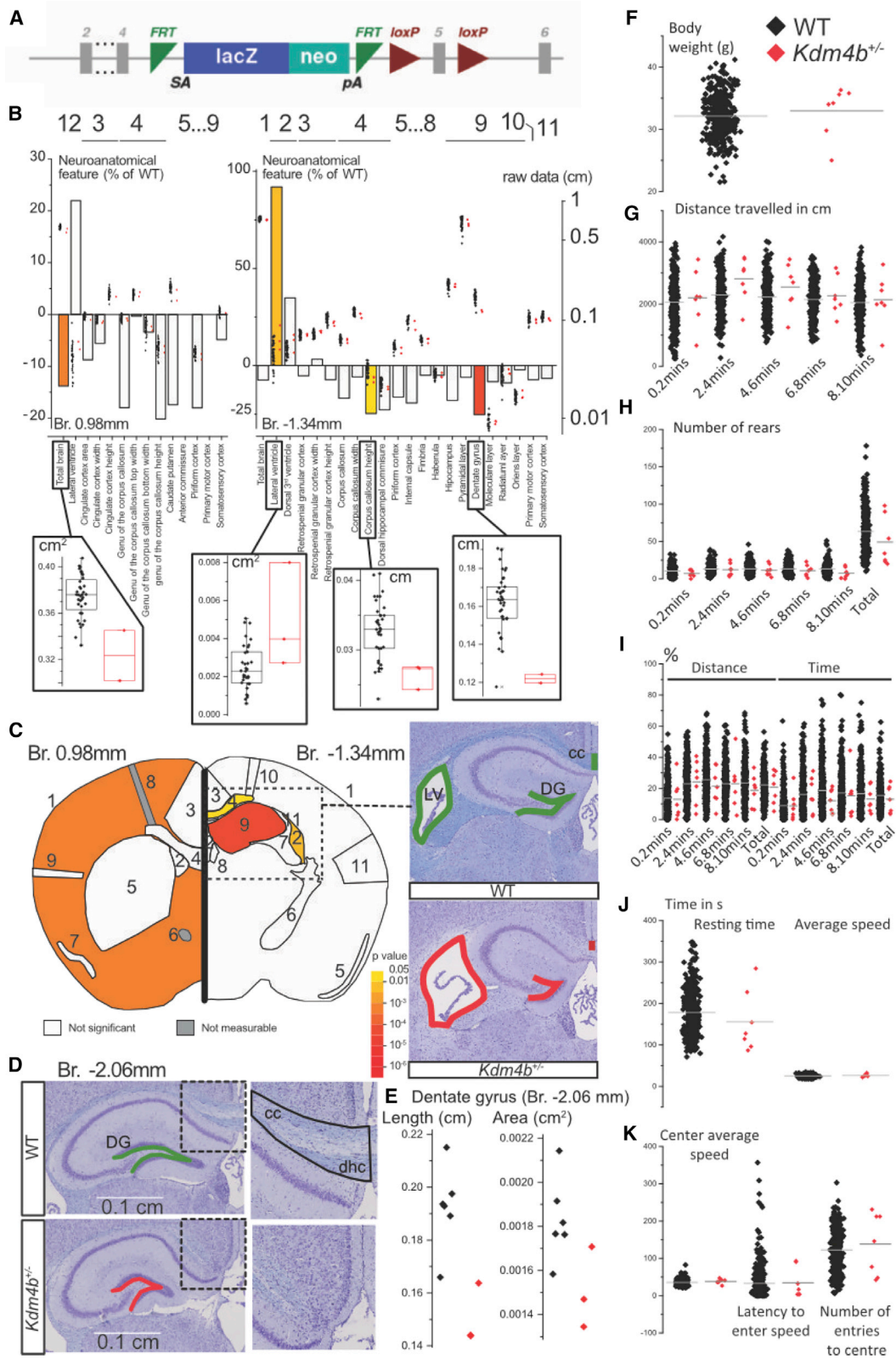


Figure 3. Mouse Studies Reveal a Role of KDM4B in the Anatomy of the Brain

(A) Construction of the *Kdm4b*^{tm1a(EUCOMM)Wtsi} allele.

(B) Histograms for three heterozygous *Kdm4b* mice showing percentage difference relative to 40 WT. The overlapping dots show actual data points. To present areas and lengths on the same scale, the square root of areas was used. Inserts are full dot and box plots of WT (black) versus *Kdm4b*^{+/-} mice (red) for each of the four significant parameters (total brain area, lateral ventricle area, corpus callosum height, dentate gyrus length).

(legend continued on next page)

alteration has previously been reported in other genetic causes of GDD as well, including X-linked ID, Down syndrome, and Fragile X syndrome, highlighting that appropriate synapse formation is critical for neurodevelopment.²⁹ We hypothesize that dendritic spines within the hippocampi may be altered in our human cohort, leading to the developmental delay.

To conclude, this study shows that variants in *KDM4B* can lead to syndromic GDD in humans, most likely through dysregulation of corticogenesis. These data provide insight into a mechanism of GDD; future studies evaluating the transcriptional targets and their signaling pathways will help to further elucidate the role of *KDM4B* in neurodevelopment.

Data and Code Availability

The published article includes all datasets generated and analyzed during this study in the Supplemental Information (Tables S3, S4, and S5).

Supplemental Data

Supplemental Data can be found online at <https://doi.org/10.1016/j.ajhg.2020.11.001>.

Acknowledgments

This work is supported by the National Institute of Arthritis and Musculoskeletal and Skin Diseases (R01AR068429-01 to P.B.A.) and by the National Institutes of Health (T32HD098061 to A.R.D.). The mouse neuroanatomical studies were supported by the French National Research Agency (ANR-18-CE12-0009 JCJC to B.Y.). We thank members of the Sanger Institute Mouse Pipelines teams (Ryan Beveridge, Damian Carragher, Jeanne Estabel, Yvette Hooks, Lee Mulderrig, Mark Sanderson, Daniel Sanger, Carl Shannon, and Elizabeth Tuck generated data used in this paper), the Research Support Facility for the provision and management of the *Kdm4b* mice, and Sylvie Nguyen for histological work. This work was also supported by Wellcome Trust grant WT098051 and Ministero della Salute, Ricerca Corrente 2019 (for E.A. and A.N.).

Declaration of Interests

M.J.G.S. and T.S.S. are employees of GeneDx. P.B.A. is on the Scientific Advisory Board of Illumina, Inc. and GeneDx. The other authors declare no competing interests.

Received: April 24, 2020

Accepted: November 2, 2020

Published: November 23, 2020

Web Resources

Human Splicing Finder, <https://www.genomnis.com/access-hsf>
MIM: 609765, <https://www.omim.org/entry/609765>

References

1. Moeschler, J.B., Shevell, M.; and Committee on Genetics (2014). Comprehensive evaluation of the child with intellectual disability or global developmental delays. *Pediatrics* *134*, e903–e918.
2. Centers for Disease Control and Prevention (CDC) (2004). Economic costs associated with mental retardation, cerebral palsy, hearing loss, and vision impairment—United States, 2003. *MMWR Morb. Mortal. Wkly. Rep.* *53*, 57–59.
3. Dikow, N., Moog, U., Karch, S., Sander, A., Kilian, S., Blank, R., and Reuner, G. (2019). What do parents expect from a genetic diagnosis of their child with intellectual disability? *J. Appl. Res. Intellect. Disabil.* *32*, 1129–1137.
4. Gilissen, C., Hehir-Kwa, J.Y., Thung, D.T., van de Vorst, M., van Bon, B.W., Willemsen, M.H., Kwint, M., Janssen, I.M., Hoischen, A., Schenck, A., et al. (2014). Genome sequencing identifies major causes of severe intellectual disability. *Nature* *511*, 344–347.
5. Vissers, L.E., Gilissen, C., and Veltman, J.A. (2016). Genetic studies in intellectual disability and related disorders. *Nat. Rev. Genet.* *17*, 9–18.
6. Makela, N.L., Birch, P.H., Friedman, J.M., and Marra, C.A. (2009). Parental perceived value of a diagnosis for intellectual disability (ID): a qualitative comparison of families with and without a diagnosis for their child's ID. *Am. J. Med. Genet. A.* *149A*, 2393–2402.
7. Wilson, C., and Krieg, A.J. (2019). *KDM4B*: A Nail for Every Hammer? *Genes (Basel)* *10*, 134.
8. Agger, K., Nishimura, K., Miyagi, S., Messling, J.E., Rasmussen, K.D., and Helin, K. (2019). The *KDM4/JMJD2* histone demethylases are required for hematopoietic stem cell maintenance. *Blood* *134*, 1154–1158.
9. Beyer, S., Kristensen, M.M., Jensen, K.S., Johansen, J.V., and Staller, P. (2008). The histone demethylases *JMJD1A* and *JMJD2B* are transcriptional targets of hypoxia-inducible factor HIF. *J. Biol. Chem.* *283*, 36542–36552.
10. Krieg, A.J., Rankin, E.B., Chan, D., Razorenova, O., Fernandez, S., and Giaccia, A.J. (2010). Regulation of the histone demethylase *JMJD1A* by hypoxia-inducible factor 1 alpha enhances

(C and D) Left: schematic representation of a section at Bregma +0.98 mm and Bregma –1.34 mm. Colored regions indicate the presence of at least one significant parameter within the brain region at the 0.05 level. White coloring indicates a p value higher than 0.05 and gray shows there is not enough data to calculate a p value. Right: illustrating example of WT and *Kdm4b*^{+/-} brain images in coronal sections double-stained for Nissl and Luxol at Bregma –1.34 (C) and Bregma –2.06 mm (D).

(E) Dot plot of the coronal section at Bregma –2.06 mm showing further characterization of the hippocampus.

(F) Body weight of seven *Kdm4b*^{+/-} and 771 baseline control mice.

(G) Distance traveled in cm in the open-field arena shown in sessions of 2 min each.

(H) Number of rears measured in the open-field arena.

(I) Distance and time in the open-field arena expressed in percentages.

(J) Resting time and average speed in the open-field test.

(K) Average speed in the center of the open-field arena, latency to enter the center, and the number of entries to the center.

- hypoxic gene expression and tumor growth. *Mol. Cell. Biol.* *30*, 344–353.
11. Xia, X., Lemieux, M.E., Li, W., Carroll, J.S., Brown, M., Liu, X.S., and Kung, A.L. (2009). Integrative analysis of HIF binding and transactivation reveals its role in maintaining histone methylation homeostasis. *Proc. Natl. Acad. Sci. USA* *106*, 4260–4265.
 12. Coffey, K., Rogerson, L., Ryan-Munden, C., Alkharaf, D., Stockley, J., Heer, R., Sahadevan, K., O'Neill, D., Jones, D., Darby, S., et al. (2013). The lysine demethylase, KDM4B, is a key molecule in androgen receptor signalling and turnover. *Nucleic Acids Res.* *41*, 4433–4446.
 13. Yang, J., Jubb, A.M., Pike, L., Buffa, F.M., Turley, H., Baban, D., Leek, R., Gatter, K.C., Ragoussis, J., and Harris, A.L. (2010). The histone demethylase JMJD2B is regulated by estrogen receptor α and hypoxia, and is a key mediator of estrogen induced growth. *Cancer Res.* *70*, 6456–6466.
 14. Mallette, F.A., Mattioli, F., Cui, G., Young, L.C., Hendzel, M.J., Mer, G., Sixma, T.K., and Richard, S. (2012). RNF8- and RNF168-dependent degradation of KDM4A/JMJD2A triggers 53BP1 recruitment to DNA damage sites. *EMBO J.* *31*, 1865–1878.
 15. Fujiwara, K., Fujita, Y., Kasai, A., Onaka, Y., Hashimoto, H., Okada, H., and Yamashita, T. (2016). Deletion of JMJD2B in neurons leads to defective spine maturation, hyperactive behavior and memory deficits in mouse. *Transl. Psychiatry* *6*, e766.
 16. Iwase, S., Lan, F., Bayliss, P., de la Torre-Ubieta, L., Huarte, M., Qi, H.H., Whetstone, J.R., Bonni, A., Roberts, T.M., and Shi, Y. (2007). The X-linked mental retardation gene SMCX/JARID1C defines a family of histone H3 lysine 4 demethylases. *Cell* *128*, 1077–1088.
 17. Lederer, D., Grisart, B., Digilio, M.C., Benoit, V., Crespin, M., Ghariani, S.C., Maystadt, I., Dallapiccola, B., and Verellen-Dumoulin, C. (2012). Deletion of KDM6A, a histone demethylase interacting with MLL2, in three patients with Kabuki syndrome. *Am. J. Hum. Genet.* *90*, 119–124.
 18. Dhar, S.S., Lee, S.H., Kan, P.Y., Voigt, P., Ma, L., Shi, X., Reinberg, D., and Lee, M.G. (2012). Trans-tail regulation of MLL4-catalyzed H3K4 methylation by H4R3 symmetric dimethylation is mediated by a tandem PHD of MLL4. *Genes Dev.* *26*, 2749–2762.
 19. Karczewski, K.J., Francioli, L.C., Tiao, G., Cummings, B.B., Alfoldi, J., Wang, Q., Collins, R.L., Laricchia, K.M., Ganna, A., Birnbaum, D.P., et al. Genome Aggregation Database (gnomAD) Consortium. *bioRxiv*. <https://doi.org/10.1101/531210>.
 20. Su, Z., Wang, F., Lee, J.H., Stephens, K.E., Papazyan, R., Voronina, E., Krautkramer, K.A., Raman, A., Thorpe, J.J., Boersma, M.D., et al. (2016). Reader domain specificity and lysine demethylase-4 family function. *Nat. Commun.* *7*, 13387.
 21. Skarnes, W.C., Rosen, B., West, A.P., Koutourakis, M., Bushell, W., Iyer, V., Mujica, A.O., Thomas, M., Harrow, J., Cox, T., et al. (2011). A conditional knockout resource for the genome-wide study of mouse gene function. *Nature* *474*, 337–342.
 22. Mikhaleva, A., Kannan, M., Wagner, C., and Yalcin, B. (2016). Histomorphological Phenotyping of the Adult Mouse Brain. *Curr. Protoc. Mouse Biol.* *6*, 307–332.
 23. Bjornsson, H.T. (2015). The Mendelian disorders of the epigenetic machinery. *Genome Res.* *25*, 1473–1481.
 24. Barco, A. (2014). Neuroepigenetic disorders: progress, promises and challenges. *Neuropharmacology* *80*, 1–2.
 25. Cotney, J., Muhle, R.A., Sanders, S.J., Liu, L., Willsey, A.J., Niu, W., Liu, W., Klei, L., Lei, J., Yin, J., et al. (2015). The autism-associated chromatin modifier CHD8 regulates other autism risk genes during human neurodevelopment. *Nat. Commun.* *6*, 6404.
 26. Weissman, J., Naidu, S., and Bjornsson, H.T. (2014). Abnormalities of the DNA methylation mark and its machinery: an emerging cause of neurologic dysfunction. *Semin. Neurol.* *34*, 249–257.
 27. Faundes, V., Newman, W.G., Bernardini, L., Canham, N., Clayton-Smith, J., Dallapiccola, B., Davies, S.J., Demos, M.K., Goldman, A., Gill, H., et al.; Clinical Assessment of the Utility of Sequencing and Evaluation as a Service (CAUSES) Study; and Deciphering Developmental Disorders (DDD) Study (2018). Histone Lysine Methylases and Demethylases in the Landscape of Human Developmental Disorders. *Am. J. Hum. Genet.* *102*, 175–187.
 28. Vogel-Ciernia, A., and Wood, M.A. (2014). Neuron-specific chromatin remodeling: a missing link in epigenetic mechanisms underlying synaptic plasticity, memory, and intellectual disability disorders. *Neuropharmacology* *80*, 18–27.
 29. Fiala, J.C., Spacek, J., and Harris, K.M. (2002). Dendritic spine pathology: cause or consequence of neurological disorders? *Brain Res. Brain Res. Rev.* *39*, 29–54.

Supplemental Data

Heterozygous Variants in *KDM4B* Lead to Global Developmental Delay and Neuroanatomical Defects

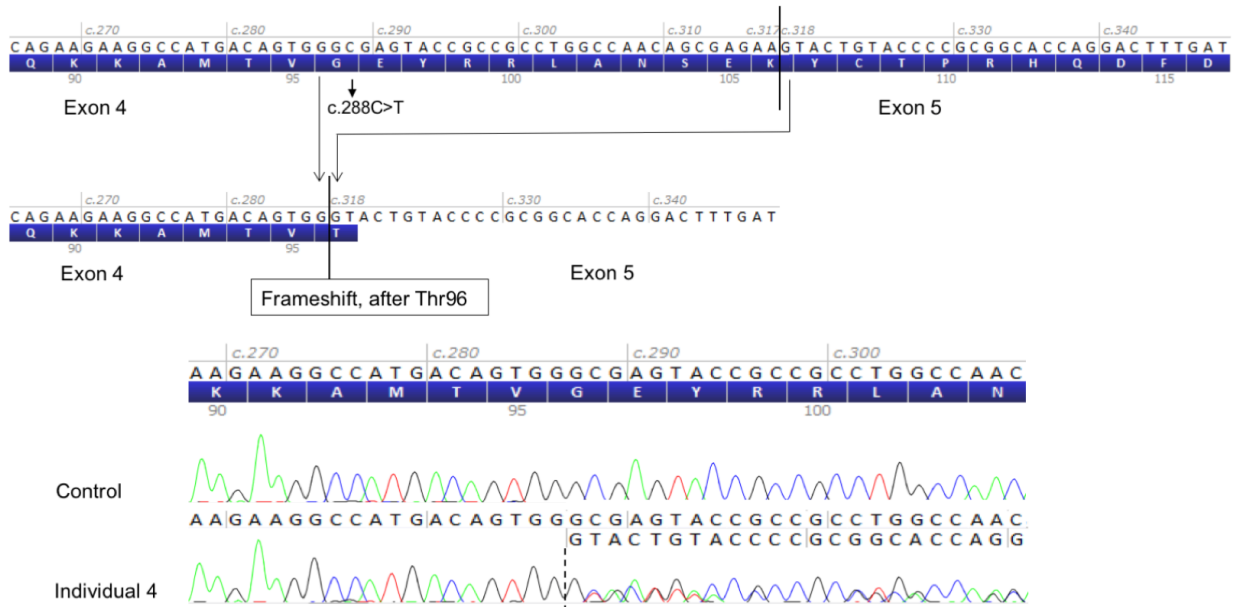
Anna R. Duncan, Antonio Vitobello, Stephan C. Collins, Valerie E. Vancollie, Christopher J. Lelliott, Lance Rodan, Jiahai Shi, Ann R. Seman, Emanuele Agolini, Antonio Novelli, Paolo Prontera, Maria J. Guillen Sacoto, Teresa Santiago-Sim, Aurélien Trimouille, Cyril Goizet, Mathilde Nizon, Ange-Line Bruel, Christophe Philippe, Patricia E. Grant, Monica H. Wojcik, Joan Stoler, Casie A. Genetti, Marieke F. van Dooren, Saskia M. Maas, Marielle Alders, Laurence Faivre, Arthur Sorlin, Grace Yoon, Binnaz Yalcin, and Pankaj B. Agrawal

SUPPLEMENTAL DATA

Supplemental Figure:

Figure S1: Synonymous variant leading altered splicing in Individual 4

Individual 4: c.(288C>T), r.(287_317del), p.(Glu97Thrfs*66)



RT PCR and sequencing data for the variant in Individual 4. RNA was extracted from peripheral blood. Variant c.288C>T creates an ectopic splice site resulting in a 31 nucleotide deletion in the mRNA r.(287_317del), and a frameshift p.(Glu97Thrfs*66).

Supplemental Table

Table S1: Dysmorphic physical features present in the clinical cohort

Individual	Dysmorphic Physical Features
1	Turricephaly, protruding metopic ridge, short philtrum, large hyperangulated ears, downturned corners of mouth, low adipose tissue in forearms and feet, dystrophic hair
2	Mild facial asymmetry, epicanthal folds, high palate
3	Synophrys, upslanting palpebral fissures, upturned tip of nose, tent shaped mouth, clinodactyly of 5th fingers, short thumbs
4	Metopic ridge present, short philtrum, sparse temporal hair, broad nasal bridge, full upper lip
5	Low posterior hair line, wide nasal bridge, downturned corners of mouth, Short hands and feet, bilateral clinodactyly of the 5th fingers and fourth toes
6	Bitemporal narrowing, narrow palpebral fissures, lowered inner canthus, large ears, Mild microstomia with tented upper lip vermillion
7	Positional plagiocephaly, short broad forehead, round face with prominent micrognathia, sparse hair, horizontal palpebral fissures, markedly thinned eyebrows, small low set posteriorly rotated ears with over-folded helices and cupped shape, short nose with anteverted nares, microstomia, long philtrum, prominent calcanei with deep-set nails
8	Anteverted nares, short philtrum
9	Synophrys, bulbous tip of nose, Robin syndrome, single palmar crease, clinodactyly of 5 th finger with P2 hypotrophy

Supplemental Methods:

Human subjects

Individual 2 was enrolled in a research study at the Manton Center for Orphan Disease Research at Boston Children's Hospital (BCH) and exome sequencing (ES) was performed by GeneDx. The study and collection of this cohort data was approved by the BCH Institutional Review Board (IRB). The *KDM4B* variant was added to GeneMatcher and 6 additional individuals were identified with *KDM4B* variants. Data for these individuals was shared in accordance with their home IRB/ REC (Research Ethics Committee).

RNA analysis of Individual 4

RNA was extracted from peripheral blood drawn in PAXgene blood tubes (Qiagen) according to the manufacturers recommendations. Reverse transcriptase was performed using Superscript III First-Strand Synthesis System for RT-PCR (Invitrogen) and random hexamers. Specific amplification of KDM4B mRNA was done using the gene specific primers, EXON3F ATCATGACGTTTCGCCCAAC and EXON5R ATCGGGGAGACAAAGGTGAG. The PCR product was sequenced using Brilliant Dye terminator v1.1 chemistry (Nimagen) and an ABI sequencer 3730 Genetic Analyzer (Illumina). Obtained sequences were analysed using CodonCode Aligner (CodonCode Corporation).

Kdm4b mouse model

The mouse model was generated by homologous recombination in embryonic stem cells using the Knockout-first allele method¹, producing the *Kdm4b*^{tm1a(EUCOMM)Wtsi} allele which were then phenotyped (Figure 3A). Mice were phenotyped by the Mouse Genetics Project (MGP) pipeline at the Wellcome Sanger Institute (UK) and were given a HFD (high fat diet) from 4 weeks of age (Western RD, 829100, 21.4% crude fat content, 42% kcal as fat, 0.2% cholesterol Special Diet Services, Witham, UK). Animal care was as previously described².

After weaning, animals were housed three to four mice per cage with WT controls housed separately, in a specific-pathogen-free environment in individually ventilated cages under 12/12 light/dark cycle with temperature-controlled conditions and free

access to food and water with hardwood bedding. All animals were regularly monitored for health and welfare concerns and were additionally checked prior to and after procedures.

Behavioral analysis

Behavioral experiments were conducted at the Wellcome Sanger Institute (UK) by a small group of operators. The open-field test encompasses studying basic locomotor activity, hyperactivity, exploratory behavior, and anxiety in mice. The mice were placed at the edge of the arena which was illuminated with dispersed light measured between 166 and 175lx. The arena measured 45.7 × 45.7 × 50cm and comprised of infrared transparent, black acrylic walls and a sandblasted grey acrylic floor (TSE Systems, Bad Homburg, Germany). The mice were monitored for 10 minutes by the ActiMot system (version 7.01) which uses a grid of 32 IR beams on each axis to locate the mice, as well as a further 32 beams on one axis, 8cm above the base of the arena, to measure rearing activity. Within the software, the arena was split into two zones: a peripheral zone of 8cm diameter from each wall and a central zone that was 42% of the area of the arena.

Data were analyzed using Acti-Track software (version 7.01). Speed and distance covered by the mice were then quantified as well as the percentage of time spent in defined zones of the field (periphery, intermediate or center). Seven male and seven female heterozygous mice were tested at 9 weeks of age. Data were analyzed using a

linear mixed model to determine whether a behavioral parameter is significantly different between the experimental groups.

Neuroanatomical studies

Neuroanatomical studies were carried out using 3 heterozygous *Kdm4b*^{+/-} and a baseline set of 40 WT mice at 16-week old as previously described³. Mice were anaesthetized with Ketamine (100 mg/kg, intraperitoneally) and Xylazine (10 mg/kg, i.p.), blood collected via the retroorbital route and death confirmed before the brains were dissected and fixed in 4% buffered formalin for a week, then transferred to 70% ethanol. Samples were embedded in paraffin using an automated embedding machine (Sakura Tissue-Tek VIP) and cut at a thickness of 5µm with a microtome in order to obtain coronal brain region at Bregma +0.98 mm, Bregma -1.34 mm and Bregma -2.06 mm. The sections were then stained with 0.1% Luxol Fast Blue (Solvent Blue 38; Sigma-Aldrich) and 0.1% Cresyl violet acetate (Sigma-Aldrich) and scanned using Nanozoomer 2.0HT, C9600 series at 20× resolution.

Seventy-two brain parameters, made up of area and length measurements as well as cell level features, were taken blind to the genotype across the three coronal sections. Data were analyzed using a linear mixed model to determine whether a brain region is associated with neuroanatomical defect or not.

Ethical considerations in animal use

The care and use of mice in the Wellcome Sanger Institute study was carried out in accordance with UK Home Office regulations, UK Animals (Scientific Procedures) Act of 1986 under UK Home Office license (80/2076) that approved this work, which was reviewed regularly by the Wellcome Sanger Institute Animal Welfare and Ethical Review Body.

Supplemental References

1. Skarnes, W.C., Rosen, B., West, A.P., Koutsourakis, M., Bushell, W., Iyer, V., Mujica, A.O., Thomas, M., Harrow, J., Cox, T., et al. (2011). A conditional knockout resource for the genome-wide study of mouse gene function. *Nature* 474, 337-342.
2. White, J.K., Gerdin, A.K., Karp, N.A., Ryder, E., Buljan, M., Bussell, J.N., Salisbury, J., Clare, S., Ingham, N.J., Podrini, C., et al. (2013). Genome-wide generation and systematic phenotyping of knockout mice reveals new roles for many genes. *Cell* 154, 452-464.
3. Mikhaleva, A., Kannan, M., Wagner, C., and Yalcin, B. (2016). Histomorphological Phenotyping of the Adult Mouse Brain. *Curr Protoc Mouse Biol* 6, 307-332.